Eur. Phys. J. B **15**, 649–656 (2000)

THE EUROPEAN PHYSICAL JOURNAL B

EDP Sciences

Magnetism and superconductivity in $Sr_2YRu_{1-u}Cu_uO_6$ and magnetism in $Ba_2GdRu_{1-u}Cu_uO_6$

H.A. Blackstead[1], John D. Dow[2,a], D.R. Harshman[1,3], M.J. DeMarco[4], M.K. Wu[5], D.Y. Chen[5], F.Z. Chien[6], D.B. Pulling[1], W.J. Kossler[7], A.J. Greer[8], C.E. Stronach[9], E. Koster[10], B. Hitti[11], M. Haka[12], and S. Toorongian[12]

[1] Physics Department, University of Notre Dame, Notre Dame, IN 46556, USA
[2] Physics Department, Arizona State University, Tempe, AZ 85287-1504, USA
[3] Physikon Research, Inc. P.O. Box 2421 Blaine, WA 98231, USA
[4] Physics Department, Buffalo State College, Buffalo, NY 14222, USA
[5] Department of Physics and Materials Science Center, National Tsing Hua University, Hsinchu, Taiwan
[6] Physics Department, Tamkang University, Tamsui, Taiwan
[7] Physics Department, College of William and Mary, Williamsburg, VA 23185, USA
[8] Physics Department, Gonzaga University, Spokane, WA 99258, USA
[9] Physics Department, Virginia State University, Petersburg, VA 23806, USA
[10] Physics Department, University of British Columbia, Vancouver, B.C., Canada V6T 1Z1
[11] TRIUMF, Vancouver, B.C., Canada V6T 2A3
[12] Nuclear Medicine Department, State University of New York, Buffalo, NY 14260, USA

Received 30 September 1999

Abstract. We report magnetization, surface resistance ($R_s(T,H)$), and electron spin resonance (ESR) for non-superconducting $Ba_2GdRu_{1-u}Cu_uO_6$, and find that all three magnetic ions (Gd, Ru, and Cu) are ordered at low temperatures. Both ESR (Gd sublattice) and weak ferromagnetic resonance (dopant Cu) are observed, while no magnetic resonance due to either paramagnetic or ordered Ru is detected. In addition, for superconducting ($T_c \sim 45$ K) $Sr_2YRu_{1-u}Cu_uO_6$, resistivity, muon spin rotation (μ^+SR), and ^{99}Ru Mössbauer absorption are reported. None of the O_6 materials (*e.g.*, $Sr_2YRu_{1-u}Cu_uO_6$) have cuprate planes, although Cu is employed as a dopant. In $Sr_2YRu_{1-u}Cu_uO_6$, the Ru moments order at a temperature (∼23 K) below that for the resistive onset of superconductivity, while the Cu orders at a higher temperature, ∼86 K. Therefore at low temperatures, this material exhibits magnetic order, coexisting with diamagnetism. The only non-magnetic layers in the superconducting O_6 structure, the SrO layers, carry holes and exhibit diamagnetic screening characteristic of type-II superconductivity.

PACS. 74.72.-h High-T_c compounds – 76.30.-v Electron paramagnetic resonance and relaxation – 76.80.+y Mössbauer effect; other γ-ray spectroscopy

1 Introduction

A new class of high temperature superconductors (HTSCs) has recently been discovered by Wu *et al.* [1,2]: materials that will play an important role in identifying the origin of superconductivity in metal-oxide systems. Contrary to popular expectations, these two-layer materials superconduct without the nearly ubiquitious CuO_2 planes usually associated with high temperature superconductivity. The two layers consist of SrO and $YRu_{1-u}Cu_uO_4$ planes, see Figure 1 [3]. In this structure, the larger Y (or Gd) ion is size-compensated, by a smaller Ru ion or by a similarly sized Cu ion at an adjacent cation site, to approximately match the Sr–O bond-length. The dopant Cu partially replaces higher valence Ru^{+5} and dopes holes into the structure. The $YRuO_4$ to $(SrO)_2$ size-match is not perfect, leaving the Sr–O bonds stretched. This bond-stretching has the impact of imparting (on average) a fraction (∼0.25) of a hole to the oxygen of the SrO layer from the $YRuO_4$ layer [4]. Moreover, RuO_2 is well-known to be a good (electron) conductor, and so we expect that these $Sr_2YRu_{1-u}Cu_uO_6$ materials, when lightly Cu-doped, will exhibit behavior similar to the cuprates: *p*-type conductivity and superconductivity (associated with holes on oxygen in the SrO layers) and *n*-type normal-metal conducting planes ($YRu_{1-u}Cu_uO_4$).

We report here a variety of experiments emphasizing the use of local probes, including the Mössbauer effect, muon spin rotation (μ^+SR), and electron spin resonance (ESR), in addition to resistivity and magnetization measurements. Temperature- and field-dependent microwave frequency surface resistance measurements ($R_s(T,H)$) were used to probe the vortex lattice on a time scale

[a] e-mail: cats@dancris.com

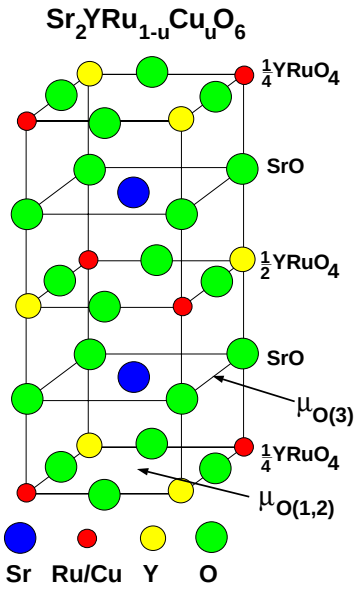

Fig. 1. Idealized structure of Sr_2YRuO_6. Here, 1/4 of the unit cell is illustrated. Y and Ru are each surrounded by oxygen octahedra. In reality (not shown in the idealized structure) the Ru–O bond lengths are shorter (∼0.26 Å) than the Y–O bond lengths, because of the comparatively smaller ionic size of Ru, and because the octahedra rotate as shown in reference [3]. This material is doped by 5–15% Cu substituted for Ru. Two nearly equivalent oxygen sites in the $YRuO_4$ layer are designated as the O(1)- and O(2)-sites, and the O(3)-site is in the SrO layer. The identified muon sites are indicated by arrows.

$\sim 10^{-10}$ s, and to demonstrate superconductivity in the presence of substantial current densities, $\sim 10^3 - 10^5$ A/cm^2, and for magnetic fields that were varied from zero to a maximum of 2 T. The μ^+SR experiments directly probed the vortex lattice on a very small length scale, and on a time scale $\sim 10^{-6}$ s, for a smaller range of applied fields. The Mössbauer experiments probed for magnetic order in the Ru sublattice.

2 Sample preparation

Polycrystalline samples of $Sr_2YRu_{1-u}Cu_uO_6$ with $u = 0.05$, 0.1, and 0.15, were prepared using standard solid-state reaction techniques. Starting powders with stoichiometric compositions of $SrCO_3$, Y_2O_3, RuO_2, and CuO were mixed thoroughly, and calcined at 1000 °C for several days in air to produce $Sr_2YRu_{1-u}Cu_uO_6$. $Ba_2GdRu_{1-u}Cu_uO_6$ was prepared similarly. Reacted powders were ground, pressed into pellets, and sintered at 1380 °C in 70%–30% O_2–Ar mixtures for 12 hours. Structural characterization was carried out by scanning electron microscopy, including energy dispersive X-ray analysis. X-ray and neutron diffraction placed an upper limit on phase inhomogeneity of less than 1%.

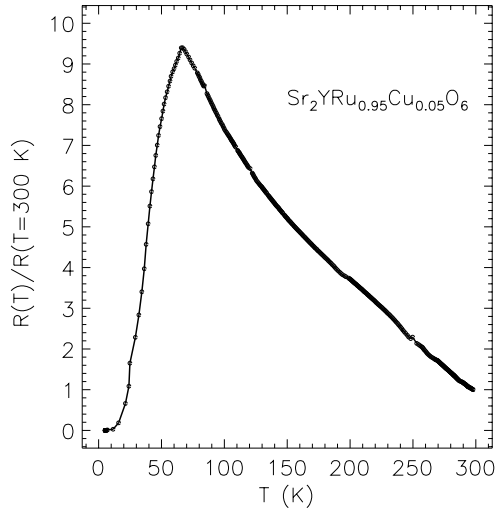

Fig. 2. Temperature-dependent normalized resistance of $Sr_2YRu_{0.95}Cu_{0.05}O_6$. These data indicate the onset of superconductivity above 45 K, followed at lower temperature by a transition with a width of ∼15 K. There is little apparent impact of the Ru ordering, which occurs at ∼23 K.

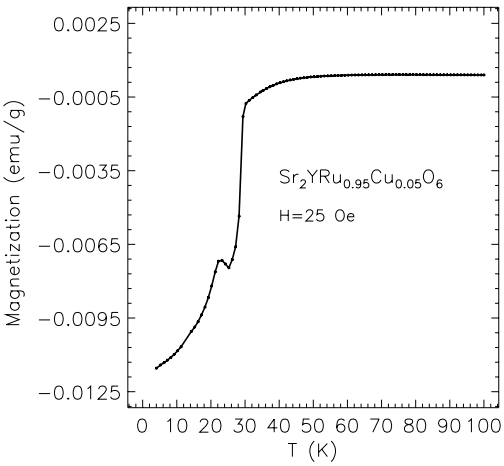

Fig. 3. Temperature-dependent magnetization of $Sr_2YRu_{0.95}Cu_{0.05}O_6$, with an applied field of $H = 25$ Oe. The peak in the magnetization at ∼23 K is due to ordering of the Ru moments. The dc resistance data (Fig. 2) may exhibit a small anomaly near this temperature.

3 Signatures of superconductivity: resistivity and magnetization of $Sr_2YRu_{1-u}Cu_uO_6$

The temperature-dependent resistance of $Sr_2YRu_{0.95}Cu_{0.05}O_6$ (see Fig. 2) is suggestive of a semiconducting response, followed at lower temperatures by superconductivity. This is typical for these materials. The zero-field cooled magnetization with $H = 25$ Oe is illustrated in Figure 3. These data have an interesting feature, a peak at ∼23 K, well below the superconducting (onset) transition temperature which is ∼45 K. This peak is due to ordering of the Ru moments, as discussed below. For temperatures below both the superconducting transition temperature and the Ru ordering temperature,

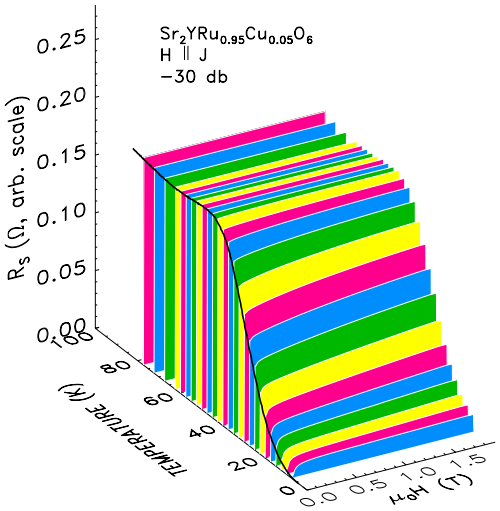

Fig. 4. Field- and temperature-dependent surface resistance (12.95 GHz) of $Sr_2YRu_{0.95}Cu_{0.05}O_6$. For $H = 0$, $R_s(H = 0, T)$ decreases slowly as T is reduced, until near 65 K, R_s begins to increase. Near ∼45 K, the onset (T_c) of superconductivity is attained. As the temperature is further reduced, R_s decreases to a very small value, ∼1 mΩ. There is evidence neither of Ru order in R_s, nor for any Ru resonant response. The incident rf power was attenuated by 30 db, to ∼100 μW.

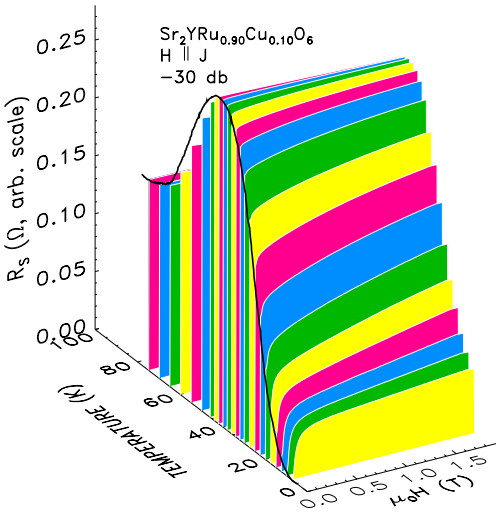

Fig. 5. Field- and temperature-dependent surface resistance of $Sr_2YRu_{0.9}Cu_{0.1}O_6$. For $H = 0$, $R_s(H = 0, T)$ increases substantially as T is reduced until ∼45 K is reached and the onset (T_c) of superconductivity is attained. This behavior with a maximum in R_s is more pronounced than with $u = 0.05$. As the temperature is further reduced, R_s approaches a small value, and there is neither evidence of Ru order, nor any Ru resonant response.

the resulting magnetization as a function of the applied field is the superposition of superconducting and antiferromagnetic responses.

4 Microwave surface resistance

4.1 $Sr_2YRu_{1-u}Cu_uO_6$

Microwave surface resistance data, as functions of temperature and applied field, for two dopant contents are illustrated in Figures 4, 5, and 6. In Figure 4, we have $u = 0.05$ (the smallest dopant content u reported here). The data indicate that the surface resistance contains three effects: (i) a normal-state field-dependent magnetoresistive response (bump above T_c), (ii) superconducting vortex dissipation $R_s(H)$ shows the characteristic increase with H below T_c, and (iii) temperature-dependent resistivity. In the normal state, we have $R_s(H, T) = (\mu_0\omega\rho(T, H)/2)^{1/2}$, ω is the angular microwave frequency, and ρ is the resistivity. The magnetoresistive response in the normal state is identified by the decrease in $R_s(H)$, as H increases, for $T < 70$ K. The vortex dissipation is characterized by a field-dependence in which the isothermal $R_s(H)$ increases roughly as $H^{1/2}$, for $T < T_c$.

In Figure 5, data for the surface resistance of a sample with $u = 0.10$ are given. As for the sample with $u = 0.05$, the surface resistance data indicate clearly the onset of superconductivity and vortex dissipation with $H > 0$. The data differ in that magnetoresistive effects are more pronounced, and compete with vortex dissipation in the superconducting state.

In Figure 6, temperature- and field-dependent surface resistance data are given for the sample with $u = 0.1$, in

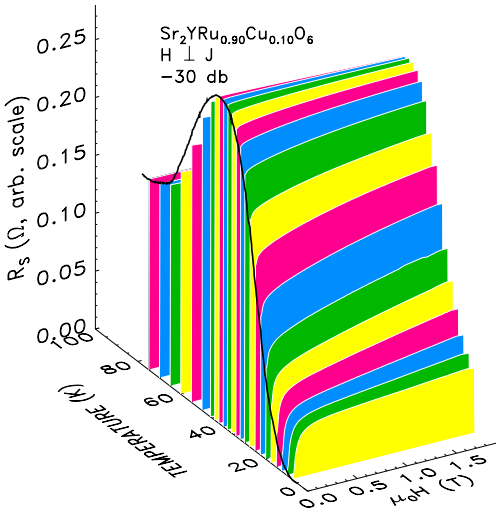

Fig. 6. Field- and temperature-dependent surface resistance of $Sr_2YRu_{0.9}$ $Cu_{0.1}O_6$. For $H = 0$, $R_s(H = 0, T)$ increases substantially as T is reduced until ∼45 K is reached and the onset (T_c) of superconductivity is attained. As the temperature is further reduced, R_s approaches a small value, and there is neither evidence of Ru order, nor any resonant response. These data are with $J_{rf} \perp H$, in the maximum Lorentz force configuration, and are very similar to those of Figure 5.

the configuration in which J_{rf} is perpendicular to H. In this configuration the magnetic resonance is minimized, and Lorentz forces on vortices are optimized. These data are nearly identical to those of Figure 5; there is no evidence for any resonance, nor is the vortex dissipation enhanced. This nearly isotropic response is consistent with pancake vortices. Magnetization, dc resistivity measurements, and μ^+SR data (see below) all confirm that Sr_2YRu_{1-u} Cu_uO_6 superconducts.

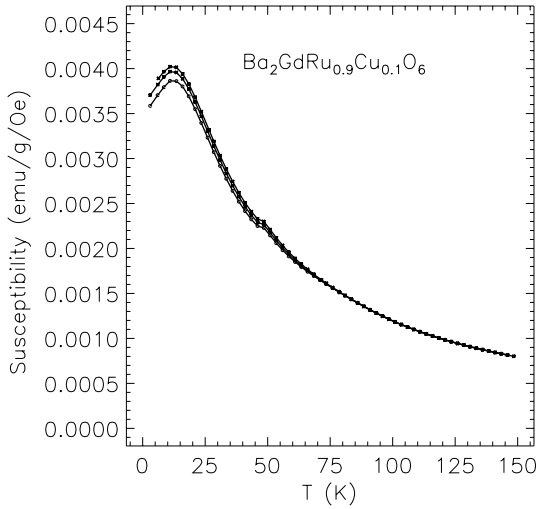

Fig. 7. Susceptibility of $Ba_2GdRu_{1-u}Cu_uO_6$, with $u = 0.1$, as a function of temperature with $H = 88$, 38 and 8 Oe. These data indicate transitions at ∼48 K (Ru) and at ∼12.5 K (Gd). The susceptibility becomes field-dependent below ∼86 K.

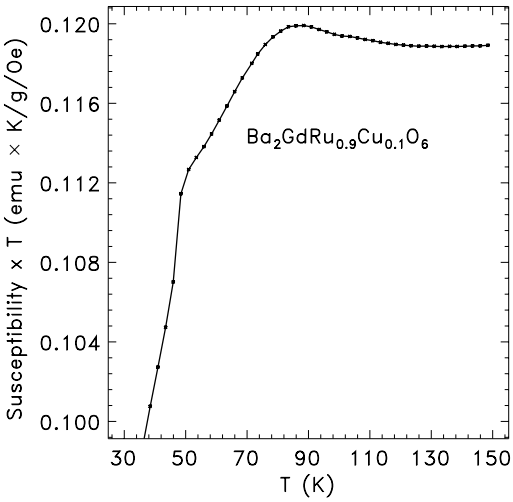

Fig. 8. Susceptibility multiplied by temperature, $\chi(T) \times T$, for $Ba_2GdRu_{1-u}Cu_uO_6$, with $u = 0.1$, as a function of temperature with $H = 88$ Oe. These data indicate a transition at ∼86 K which vanishes with $u = 0$, identifying Cu as the ordered ion.

The surface resistance measurement technique utilizes large current densities, $\sim 10^3 - 10^5$ A/cm^2. The minimum current density in our apparatus is $\sim 10^3$ A/cm^2, proving that these materials (with the several dopant levels u) are robust superconductors.

4.2 $Ba_2GdRu_{1-u}Cu_uO_6$

Replacing Y with Gd, and Sr with Ba in $Sr_2YRu_{1-u}Cu_uO_6$ yields a structural homologue, $Ba_2GdRu_{1-u}Cu_uO_6$. Figure 7 illustrates the magnetic susceptibility $\chi(T)$ of a sample with $u = 0.1$. These data indicate two magnetic transitions at ∼48 K (associated with the Ru sublattice) and ∼12.5 K (associated with the Gd sublattice). The presence of a third transition (at ∼86 K) is revealed by plotting the susceptibility data $\chi(T) \times T$, see Figure 8. The data in Figure 8 clearly show that the susceptibility deviates from paramagnetic dependence at ∼86 K (due to Cu).

4.2.1 Gd ESR as a local probe

In Figure 9, microwave data are presented. The sharp peak at approximately 0.464 T is the Gd electron spin resonance (ESR), which in our experience is unusually narrow; this may be a consequence of exchange narrowing [5]. At the highest temperatures illustrated, the Gd ESR line-shape is symmetric, with no indication of the asymmetry due to a Dysonian line-shape [6] characteristic of ESR in a metal. The Gd ESR response broadens dramatically as the temperature decreases and effectively disappears for temperatures below ∼48 K, a temperature that corresponds closely with a peak in the susceptibility (Fig. 7). There are potentially quite a number of magnetic scenarios for explaining these behaviors, and at this time it is not possible to select among them with complete reliability. Nevertheless, certain features are clear and unambiguous: (i) At high temperatures ($T > 86$ K), all the magnetic ions (Gd, Ru, and Cu) are paramagnetic, as was demonstrated by the linearity of the magnetization in H. The paramagnetic Ru moment, deduced from these data, is quite small, ∼0.3 μ_B. (ii) The Gd moments are not ordered between 86 K and ∼48 K, because the integrated intensity of the resonance varies faster than $1/T$ in this temperature range, while the resonance line-width increases. (iii) While it is conceivable that the Gd orders at ∼48 K, it is the case that the Ru orders instead, and consequently the Gd spins are subjected to large local exchange and dipole fields which cause extreme broadening of the Gd ESR. Doi and Hinatsu [3] argue that rare-earth magnetic interactions are comparatively weak in Sr_2LnRuO_6 (Ln = lanthanide) materials. They also note that the paramagnetic moment of Ru in these materials is small, in agreement with our observations above 86 K. These authors also report the temperature-dependent susceptibility of the homologue Sr_2GdRuO_6, finding ordering only at low temperatures, ∼10 K. It seems evident that inclusion of the dopant Cu has an impact on the magnetic behavior, ordering at ∼86 K.

Exchange narrowing [5] arising from coupling to the Ru-spins is the likely source of the narrow high-temperature Gd ESR line-width. It also seems unlikely that Gd undergoes antiferromagnetic ordering at temperatures as high as ∼48 K; this temperature is much higher than the well-known $T_N = 2.2$ K ordering in $GdBa_2Cu_3O_7$. It is also possible to rule out ferromagnetic Gd. Ferromagnetic resonance would be readily detectable at this rf frequency (12.95 GHz), and the impact of demagnetizing fields would be in evidence: Gd is an $L = 0$ ion with very small single ion anisotropy contributing to the $q = 0$ magnon energy gap; Gd ferromagnetic resonance would be unobservable only if the $q = 0$ magnon energy gap were to exceed the microwave photon energy ($\hbar\omega_{magon}(q = 0) > \hbar\omega_{photon}$). A similar argument also

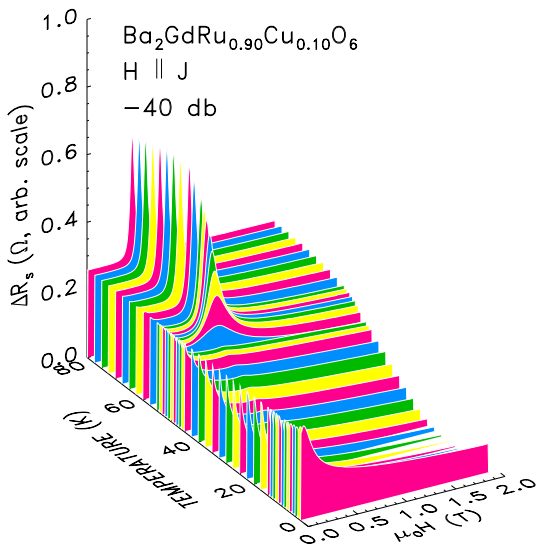

Fig. 9. Field-induced changes in the temperature-dependent surface resistance, $\Delta R_s(T,H) = R_s(T,H) - R_s(T,H=0)$. These data include a very narrow Gd ESR signal at an applied field of ∼0.46 T. This resonance broadens to near undetectability below ∼48 K. There is a second (weak ferromagnetic) resonance observed at very small fields, which appears near 60 K, shifts slowly to higher fields, and persists to the lowest temperatures. This low field resonance is attributed to Cu.

rules out antiferromagnetic Gd ordering at ∼48 K. (These arguments would be altered if the Gd and Ru moments order ferrimagnetically at ∼48 K and re-order at ∼12.5 K.)

In Sr_2HoRuO_6, Ho and Ru order ferrimagnetically [7], with a simple planar $(a-b)$ structure. Each of the magnetic sublattices, Ru and Ho, orders ferromagnetically, but the direction of the net ferrimagnetic magnetization alternates from magnetic layer to magnetic layer, producing an overall antiferromagnetic structure. It seems likely that the Gd homologue studied here has a similar magnetic structure at low temperatures, but the large Gd neutron absorption cross-section prohibits the appropriate experiments for determining this without use of a low cross-section Gd isotope.

4.2.2 Cu resonance

There is another resonance signal in addition to the Gd ESR. This resonance occurs at very low fields, and in two rf–dc magnetic field configurations, $H_{rf} \perp H_{dc}$ and $H_{rf} \parallel H_{dc}$. This is the signature either of antiferromagnetic resonance or of weak ferromagnetic resonance [8], and not ferromagnetic or paramagnetic resonance. The temperature below which this resonance is first observed is 60 K (in both $Ba_2GdRu_{1-u}Cu_uO_6$ and $Sr_2YRu_{1-u}Cu_uO_6$) [9]. Since this signal vanished for $u = 0$ (no Cu), it is due to ordered Cu.

In several other Ru-containing materials for which we have carried out detailed rf studies, there was no evidence for a Ru resonant response, whether ordered or disordered. It is noted that Ru ESR has been reported in several systems [10] in which Ru is present in dilute content, and the Ru^{+5} magnetic moment is well-localized. Our failure to detect Ru resonance is likely a consequence of itinerancy which leads to rapid relaxation and an extremely broad (undetectable) line width. Thus, the low field resonance signal at and below 60 K is due to ordered Cu [9]. The lack of a noticeable peak in the susceptibility (Fig. 7) at ∼86 K may be consistent with the relatively small dopant content, and the weak ferromagnetic order. It follows that the ordering at ∼48 K must be the Ru sublattice, and the ordering at ∼12.5 K is likely the Gd sublattice.

Another possibility is that the magnetic ordering may be more complex, involving ferrimagnetic coupling. While the dc resistivity data (not shown) have suggested superconductivity with $T_c \sim 50$ K, the microwave response detects neither a resistive drop at ∼50 K, nor a drop at low temperatures, nor vortex dissipation. Unlike in $Sr_2YRu_{1-u}Cu_uO_6$, neither the magnetization data nor the microwave surface resistance data are consistent with superconductivity in $Ba_2GdRu_{1-u}Cu_uO_6$ [11–13].

5 Muon spin rotation in $Sr_2YRu_{1-u}Cu_uO_6$

The crystal structure of $Sr_2YRu_{1-u}Cu_uO_6$ (Fig. 1) contains three inequivalent O-sites, which were studied with muon spin rotation. Two of the sites, denoted O(1) and O(2), are in the $YRu_{1-u}Cu_uO_4$ layer, and the other (O(3)) is in the SrO layer. The nearly equivalent O(1) and O(2)-sites differ because of the size and chemical disparity of Ru and Y (not shown in the idealized structure in Fig. 1). As a consequence of the local-probe character of the μ^+SR technique, it was found possible to determine the hole location and to directly observe Meissner screening.

The positive muons (μ^+) come to rest in proximity to negatively charged oxygen; two muon sites are available. One muon site is formed by four oxygen ions (two O(1) and two O(2)) in the $YRu_{1-u}Cu_uO_4$ layer, designated the $\mu_{O(1,2)}$-site. The second site, associated with the SrO layer and designated the $\mu_{O(3)}$-site, is also formed by four oxygen, two O(3), and an O(1) and an O(2). The volume available to the muon at each of these two sites is roughly commensurate with the size of muonium. In the following, we show how each of the two muon sites has uniquely identifiable characteristics.

The time-differential μ^+SR technique employed in these measurements is described in detail elsewhere [14,15], and only a brief overview will be given here. The spectrometer employed has been designed to eliminate virtually all background signals from the sample holder, etc. This feature facilitated recovery and separation of a minority signal.

Positive (∼4.2 MeV) muons produced at the TRIUMF accelerator with their spins aligned antiparallel to their momenta are stopped in the sample, where they decay (∼2.2 μs half-life) yielding a positron and an undetected neutrino-antineutrino pair. The positrons are preferentially emitted along the direction of the muon spin. Since the muon precesses in the local magnetic field (if any) at

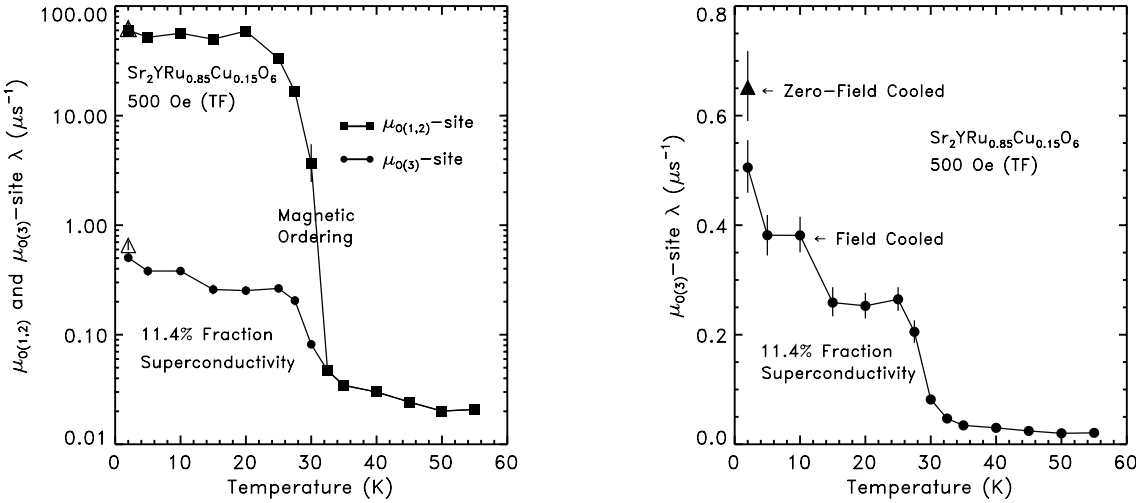

Fig. 10. Muon relaxation rate λ(T) for the $\mu_{O(1,2)}$-site (squares) in the $YRu_{1-u}Cu_uO_4$ layer (left panel, semi-log scale) and for the $\mu_{O(3)}$-site (circles) in the SrO layer (left and right (linear scale) panels) of $Sr_2YRu_{1-u}Cu_uO_6$ with $u = 0.15$. The datum indicated by the triangle in each case was obtained by zero-field cooling with subsequent application of the 500 Oe transverse field.

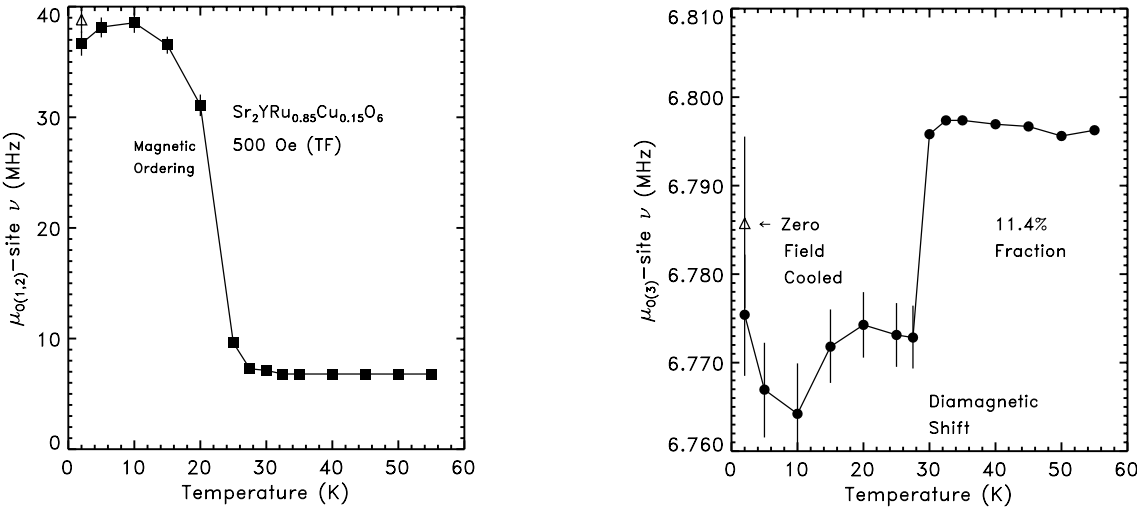

Fig. 11. Muon precession frequency data *versus* temperature, $\nu(T)$, for $Sr_2YRu_{1-u}Cu_uO_6$ with $u = 0.15$. The datum indicated by the triangle in each case was obtained by zero-field cooling (ZFC) and subsequent application of the 500 Oe field. The $\mu_{O(1,2)}$-site data indicate that Ru ions order below 30 K. The $\mu_{O(3)}$-site data show a diamagnetic shift resulting from superconductivity.

the site in which it has been thermalized, the direction of the positron carries information about the local magnetic field. Since the muons are positive, the final stopping site (with significant probability) will be a muon-site (either $\mu_{O(1,2)}$ or $\mu_{O(3)}$) formed from the more negatively charged oxygen. Thus, the signal from the O-site with (on the average) part of a hole carrier (as we shall see, $\mu_{O(3)}$) will be less intense than that for a fully charged O^{-2}-site ($\mu_{O(1,2)}$).

Measurements in both zero field (ZF) and in an applied transverse field (TF) of 500 Oe were carried out; see Figures 10 and 11.

In zero field, the data (∼90% of the muon ensemble) attributed to the $\mu_{O(1,2)}$-site exhibited a fast relaxation in a large local magnetic field (∼3000 G), while $\mu_{O(3)}$-site data (∼10% of the muon ensemble) were characterized as experiencing a negligible magnetic field and exhibited no relaxation.

We find that this combination of fields (0 G and ∼3000 G) cannot be achieved with a spin configuration that leads to a zero field at the $\mu_{O(1,2)}$-site because for such a spin configuration the field at the $\mu_{O(3)}$-site also vanishes, contrary to the observation that one of these two sites has a ∼3 kG field. The only type of magnetic order consistent with our measurements is an ordered configuration of Ru-moments in the $a-b$ plane: The observed size of the field at the $\mu_{O(1,2)}$-site is consistent with ferromagnetic order in the sheets, and the observed zero value of $\mu_{O(3)}$ is consistent with adjacent sheets being ordered antiferromagnetically.

In addition, the ordered Ru moment must be ∼2 μ_B. This is precisely the result obtained in recent neutron

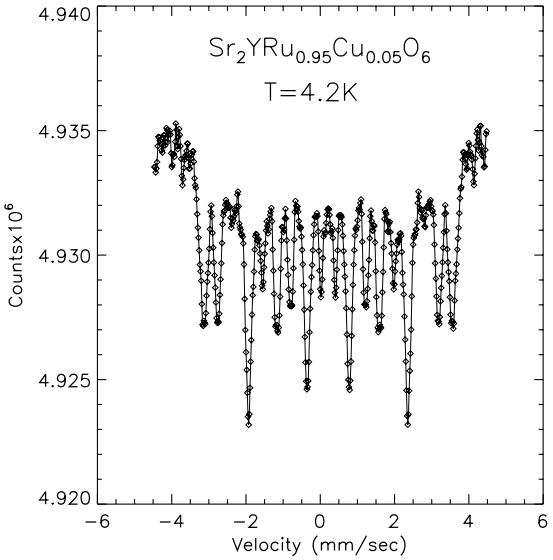

Fig. 12. Mössbauer absorption spectra at 4.2 K in $Sr_2YRu_{1-u}Cu_uO_6$, with $u = 0.05$. The data indicate magnetic order. At higher temperatures, 23–30 K, the spectrum collapses to a single line indicating a disordered system. The isomer shift indicates that the Ru is pentavalent.

diffraction studies [16], and studies carried out by Battle and Macklin [17] on undoped materials. In addition, bond-valence-sum calculations identify the O(3) site in the SrO layer as undercharged. Thus, both the magnetic characters and the average (negative) ionic charges of the O(1) and O(2) sites are consistent with these identifications.

The rapid relaxation (at low temperatures) characteristic of the $\mu_{O(1,2)}$-site data indicates magnetic disorder, which may be a consequence of dopant Cu. The data show that the abundant Ru-spins tend to "freeze" below ∼30 K, consistent with both the magnetization data and the Mössbauer data to be discussed below. The μ^+SR experiments are unable to draw any conclusions relative to ordering of the less-abundant Cu-spins. With application of an external magnetic field of 500 Oe, the $\mu_{O(1,2)}$-site in the layer $YRu_{1-u}Cu_uO_4$ exhibits a large magnetic field and rapid muon spin depolarization. At low temperatures, the $\mu_{O(3)}$-site in the SrO layer features an order of magnitude increase of the spin depolarization and a diamagnetic shift indicating superconductivity. The data for $u = 0.15$ are illustrated in Figures 10 and 11. The triangles represent data taken in transverse field, subsequent to cooling in zero field. The increase in the muon relaxation rate λ at 2 K indicates the presence of a vortex lattice. (No such shift was observed on the $\mu_{O(1,2)}$-site.) Thus, the μ^+SR evidence indicates that the $\mu_{O(3)}$-site associated with the SrO layer hosts both hole carriers and superconductivity.

6 Mössbauer spectroscopy of $Sr_2YRu_{1-u}Cu_uO_6$

A direct, independent, and unambiguous method for determination of the Ru spin-ordering temperature was obtained by utilization of ^{99}Ru Mössbauer measurements [18] to determine the hyperfine field at the Ru nucleus as a function of temperature. In addition, the valence of the Ru ion was determined by the isomer shift to be Ru^{+5} [19]; this information is critically important to determining the number of holes and to certain models of superconductivity in Ru-based materials.

^{99}Ru Mössbauer measurements require a ^{99}Rh γ-source (89 keV, 14.1 day half-life) of high chemical purity. Such a source was prepared at the cyclotron at the State University of New York at Buffalo and was used for the experiments described here.

We did not substitute ^{57}Fe for Ru in our Mössbauer experiments to determine the Ru ordering temperature [20], because such an approach invariably leads to questions concerning Fe clumping and other potentially complicating issues. Thus, doping with ^{57}Fe will likely yield interesting but potentially controversial results.

^{99}Ru Mössbauer absorption measurements described in detail elsewhere were carried out at several temperatures; data for $T = 4.2$ K are illustrated in Figure 12. These data contain the 18-line spectrum due to the mixed multipole transitions, characteristic of Ru, which results from a nuclear spin-5/2 to spin-3/2 excitation. Here, the raw data were three-point averaged twice and autocorrelated. The hyperfine field determined from the line splitting was 59.57 T, and the isomer shift was consistent with a Ru^{+5} ion [21], not with either Ru^{+4} or Ru^{+6}; which would have been readily identified [22]. There was no evidence for significant quadrupole splitting. Also, these ∼60 T hyperfine field data were characteristic of the hyperfine field ($B_{\rm hyperfine}$) of Ru^{+5}; there was no evidence for Ru^{+4}, which typically has a $B_{\rm hyperfine}$ ∼36 T. Measurements at higher temperatures (not shown) indicated that the Ru ions order magnetically between 23 K and 30 K. This result is consistent with both the magnetization measurements and the μ^+SR data.

7 Summary

The observation of superconductivity and ordered magnetism in the same unit cell in a high-temperature superconducting material is not without precedent. In the (Rare-Earth)$Ba_2Cu_3O_7$ (R123) materials, antiferromagnetic order at the R-site is well-known to occur at low temperatures without any impact on the superconductivity. In the present case, magnetic ordering occurs at a much higher temperature relative to the superconducting transition temperature, and the antiferromagnetic structure is produced by ferromagnetic (probably ferrimagnetic in the Gd material) layers in which the magnetization alternates in direction, not by antiferromagnetic layers.

The impact of magnetism on the superconductivity of $Sr_2YRu_{1-u}Cu_uO_6$ may be subtle. For example, the μ^+SR data show fully developed bulk superconductivity only below the Ru magnetic ordering temperature of ∼23 K. This ordering occurs at temperatures substantially below the superconducting onset temperature of ∼45 K. The μ^+SR experiments also determined the field at the two muon sites, finding the $\mu_{O(1,2)}$-site to have a large field

$\sim$3000 Oe, while the $\mu_{O(3)}$-site in the SrO layer exhibits a vanishingly small effective field in the ordered state. Since Ru (and dopant Cu) are the only magnetic ions in the material, unique site identification is unambiguous. The same experiments also find Meissner screening on the $\mu_{O(3)}$-site below $\sim$30 K.

It is apparent that the magnetic moments order in the $a-b$ plane, with the magnetization alternating in direction from magnetic layer to magnetic layer. This leaves the $\mu_{O(3)}$-site in a region in which the magnetic fields originating in adjacent layers tend to cancel. The microwave experiments find vortex dissipation with conventional magnetic field dependence, but with somewhat unusual dependence on the angle between $J_{\rm rf}$ and $H_{\rm dc}$. In these experiments, the vortex dissipation was almost independent of this angle, a result that we have only occasionally observed in cuprate superconductors. In this situation, the vortices characteristic of these materials must be an extreme form of the "pancake" type, existing in a single SrO layer. This interpretation is completely consistent with the μ^+SR data which exhibit extremely weak pinning, suggesting isolated sheets of "pancake vortices".

In conclusion, $Sr_2YRu_{1-u}Cu_uO_6$ superconducts, exhibiting the requisite diamagnetism, resistivity, surface resistance, and vortex dissipation characteristic of a type-II superconductor.

The $YRu_{1-u}Cu_uO_4$ layer does not exhibit type-II superconductivity, as is clearly shown by the following: (i) the Mössbauer spectra for Ru (and the magnetization data) show ordering at a temperature of $\sim$23 K which occurs below the superconducting onset temperature $\sim$45 K, and this ordering co-exists with the superconductivity at all temperatures below $\sim$23 K; and (ii) the muon spectra indicate magnetic ordering in the $YRu_{1-u}Cu_uO_4$ layer at the same temperature of $\sim$23 K, with a large magnetic field (normally inconsistent with superconductivity), and no evidence of the diamagnetic screening expected for a type-II superconductor.

The SrO layer exhibits zero net magnetic field (generally considered favorable for type-II superconductivity), and diamagnetic screening. This layer also contains the hypocharged oxygen with the holes necessary for superconductivity [23].

These facts indicate that the superconducting hole condensate is in the SrO layer and support the thesis previously advanced by two of us [24–26] that, in other materials (such as $PrBa_2Cu_3O_7$, $NdBa_2Cu_3O_7$ and $Nd_{2-z}Ce_zSr_2Cu_2NbO_{10}$), the primary superconducting condensate is not in the cuprate planes.

The authors thank S.R. Kreitzman, D. Arseneau, and M. Good for technical support. H.A.B. thanks the U.S. Department of Energy (MISCON Grant No. DE-FG0290ER45427). J.D.D. thanks the U.S. Army Research Office (Contract DAAG55-97-1-0387) and the U.S. Office of Naval Research (Contract N00014-98-10137). M.K.W., D.Y.C., and F.Z.C. gratefully acknowledge the support of ROC National Science Grant NSC87-2212-M-110-006. M.J. DeM. acknowledges support from Cottrel Research Grant (No. CC4328). C.E.S. thanks the US Air Force Office of Scientific Research for support through Grant No. F49620-97-1-0297. This research was supported in part by Physikon Research Inc. Project PL11-206.

References

1. M.K. Wu, D.Y. Chen, F.Z. Chien, S.R. Sheen, D.C. Ling, C.Y. Tai, G.Y. Tseng, D.H. Chen, F.C. Zhang, Z. Phys. B **102**, 37 (1997).
2. D.Y. Chen, F.Z. Chien, D.C. Ling, J.L. Tseng, S.R. Sheen, M.J. Wang, M.K. Wu, Physica C **282-287**, 73 (1997).
3. Y. Doi, Y. Hinatsu, J. Phys. Cond. Matter **11**, 4813 (1999).
4. Since the chemical unit cell includes $(SrO)_2$, the doping level is $\sim$0.5 hole/unit cell, a value typical of cuprate superconductors.
5. C. Kittel, E. Abrahams, Phys. Rev. **90**, 238 (1953).
6. F.J. Dyson, Phys. Rev. **98**, 349 (1955).
7. P.D. Battle, C.W. Jones, F. Studer, J. Solid State Chem. **90**, 302 (1991).
8. E.A. Turov, *Magnetic Resonance in Ferromagnetics and Antiferromagnetics as Excitation of Spin Waves* in *Ferromagnetic Resonance*, edited by S.V. Vonsovskii (Pergamon Press, Oxford, 1966), pp. 78-126.
9. Recent neutron diffraction measurements on $Sr_2YRu_{0.85}Cu_{0.15}O_6$ indicate the Cu ordering temperature to be $\sim$ 86 K, the same as for Cu in $Ba_2GdRu_{0.9}Cu_{0.10}O_6$. H.A. Blackstead, J.D. Dow. D.R. Harshman, W.B. Yelon, M.X. Chen, M.K. Wu, D.Y. Chen, F.Z. Chien, D.B. Pulling (to be published.)
10. P.G. Clem, D.A. Payne, W.L. Warren, J. Appl. Phys. **77**, 5865 (1995).
11. We note that Gd is an $L = 0$ ion, not subject to crystal field splitting, and so should suppress the superconductivity by magnetic pair-breaking.
12. H.A. Blackstead, J.D. Dow, Phys. Rev. **55**, 6605 (1997).
13. H.A. Blackstead, J.D. Dow, Phys. Lett. A **226**, 97 (1997).
14. A. Schenck, *Muon Spin Rotation Spectroscopy* (Hilger, Bristol, 1985).
15. S.F.J. Cox, J. Phys. C **20**, 3187 (1987).
16. D.Y. Chen, M.K. Wu, C.-H. Du, P.D. Hatton, F.Z. Chien, C. Ritter (to be published).
17. P.D Battle, W.J. Macklin, J. Solid State Chem. **52**, (1984) 138.
18. O.C. Kistner, Phys. Rev. **144**, 1022 (1966).
19. N.N. Greenwood, T.C. Gibb, *Mössbauer Spectroscopy* (Chapman and Hall Ltd., 1971), p. 503.
20. T.C. Gibb, R. Greatrex, N. Greenwood, K. Snowdon, J. Solid State Chem. **14**, 193 (1975).
21. M. DeMarco, D. Graf, J. Rijssenbeek, R.J. Cava, D.Z. Wang, T. Tu, Z.F. Ren, J.H. Wang, M. Haka, S. Toorongian, M. Leone, M.J. Naughton, Phys. Rev. B **60**, 7570 (1999).
22. M. DeMarco, D. Graf, J. Rijssenbeek, R.J. Cava, M. Haka, S. Toorongian, M. Leone, M.J. Naughton (to be published).
23. J.C. Phillips, Philos. Mag. B **79**, 1477 (1999).
24. H.A. Blackstead, J.D. Dow, Phys. Rev. B **51**, 11830 (1995).
25. H.A. Blackstead, J.D. Dow, Solid State Commun. **96**, 313 (1995).
26. H.A. Blackstead, J.D. Dow, Phys. Rev. B **57**, 10798 (1998).